ASCE

Size Effect on Strength Statistics of Prenotched Quasibrittle Structures

Jan Eliáš[1] and Jia-Liang Le, M.ASCE[2]

Abstract: This paper presents a stochastic analysis of the size effect on the nominal strength of quasibrittle structures with a large preexisting notch. This type of scaling behavior has been extensively studied within a deterministic framework. Little attention is paid to stochastic analysis, which is essential for reliability-based analysis and design of engineering structures. Stochastic finite element simulations are performed to study the failure of geometrically similar beams of different sizes. The numerical analysis uses a continuum damage model, in which the tensile strength and fracture energy are modeled by homogeneous random fields. Different correlation lengths are considered as a parametric study. The analysis yields the size effects on the mean and coefficient of variation (CoV) of the nominal structural strength. It is shown that the size effect on the mean strength agrees well with the Bazant size effect model. The simulation predicts a strong size effect on the CoV of the nominal strength. Small-, intermediate-, and large-size asymptotes are derived analytically for the scaling behavior of the strength CoV. Based on these asymptotes, an approximate scaling equation is proposed for the CoV of nominal strength. The effect of the correlation length on the simulated failure behavior is discussed. **DOI: 10.1061/JENMDT.EMENG-7629.**

Introduction

Over the past four decades, significant research efforts have been devoted toward the understanding of damage and fracture behaviors of structures made of brittle heterogenous materials, also known as quasibrittle materials. One important discovery is that quasibrittle structures exhibit a size dependent failure behavior, which is best manifested in terms of the size effect on the nominal structural strength (Bažant and Planas 1998; Bažant 2004, 2005; Bažant et al. 2021). Thus far, two types of size effects on the mean nominal strength have been identified: (1) Type 1 size effect, which applies to structures failing under controlled loads at macrocrack initiation; and (2) Type 2 size effect, which applies to structures of positive geometry with a preexisting large notch. The Type 1 size effect is understood to be of energetic-statistical nature, where the scaling behavior for small- and intermediate-size ranges can be derived from nonlinear fracture mechanics, and the larger-size limit follows the Weibull statistics (Bažant 2005; Bažant and Le 2017; Bažant et al. 2021). Alternatively, the Type 1 size effect can also be derived from the finite weakest-link model in a pure probabilistic framework (Bažant and Pang 2006; Bažant et al. 2009; Le et al. 2011; Bažant and Le 2017). The Type 2 size effect can be derived from an equivalent linear elastic fracture mechanics model (Bažant 2004, 2005).

Though the Type 2 size effect has been extensively investigated theoretically, numerically, and experimentally, e.g., Bažant (1984, 2004) and Bažant et al. (2021), almost all of the previous studies were cast in a deterministic setting. This is because, for structures with a preexisting notch, the location of the damage initiation cannot be random due to the stress concentration at the notch tip. Therefore, it is believed that the mean behavior of this size effect is of deterministic nature. Nevertheless, reliability-based structural design requires the knowledge of the mean behavior and, at minimum, the second-order statistics of the structural strength. A recent numerical study on diagonal shear failure of reinforced concrete beams showed a Type 2 size effect on the mean strength as well as a pronounced size effect on the variance of the structural strength (Luo et al. 2021). This result has profound implications for the safety factors used in the structural design (Le 2015; Le and Bažant 2020). However, the study covered a limited size range only, which does not reveal the entire size effect behavior. Meanwhile, in the numerical analysis, the the size of the finite-element mesh was considered to be larger than the correlation length of the random field of material properties; therefore, the influence of the correlation length on the scaling behavior was not studied.

The derivation of deterministic Type 2 size effect is anchored by the condition of positive geometry, which states that $\partial K_I/\partial a > 0$, where K_I is the stress intensity factor, and a is the crack length. Since the fracture energy is a constant over the entire crack ligament, the positive geometry implies that the crack will start to propagate as soon as the peak load is attained. In the probabilistic analysis, it is natural to introduce spatial randomness of the fracture energy. In such a case, $\partial K_I/\partial a > 0$ alone does not guarantee the absence of traction-free crack propagation at the peak load. Instead, in the mean sense, traction-free crack growth would occur. This phenomenon has recently been reported in the fracture experiments on prenotched rock specimens (Fakhimi et al. 2017).

The existence of the traction-free crack growth at the peak load poses new questions on the scaling behavior of structural strength, even for the limiting case of linear elastic fracture mechanics (LEFM). Abundant experiments on quasibrittle materials have shown that, at the limit of LEFM, the size effect on the nominal strength of geometrically similar specimens follows the $-1/2$ power law (Bažant 2004; Bažant et al. 2021). For the materials used in these experiments, the fracture toughness is expected to exhibit some spatial variation due to material

[1]Professor, Institute of Structural Mechanics, Faculty of Civil Engineering, Brno Univ. of Technology, Veveri 331/95, Brno 60200, Czechia.

[2]James L. Record Professor, Dept. of Civil, Environmental, and Geo-Engineering, Univ. of Minnesota, 500 Pillsbury Dr. S.E., Minneapolis, MN 55455 (corresponding author). ORCID: https://orcid.org/0000-0002-9494-666X. Email: jle@umn.edu

Note. This manuscript was submitted on October 20, 2023; approved on December 27, 2023; published online on March 26, 2024. Discussion period open until August 26, 2024; separate discussions must be submitted for individual papers. This paper is part of the ***Journal of Engineering Mechanics***, © ASCE, ISSN 0733-9399.

heterogeneity. In the conventional deterministic analysis, the peak load can be calculated by setting $K_I(a_0) = K_{Ic}$, where $K_I(a_0) = \sigma_N\sqrt{D}k(\alpha_0)$, wherein a_0 is the initial crack length, σ_N is the nominal structural strength, $\alpha_0 = a_0/D$ is the relative initial crack length, D is the characteristic structure size, and K_{Ic} is the fracture toughness. For geometrically similar specimens, a_0 is the constant; therefore, the nominal strength would scale with the specimen size by $D^{-1/2}$. In the probabilistic analysis, the traction-free crack growth needs to be taken into account when determining the peak load. The experimentally observed $-1/2$ scaling law implies that the length of the traction-free crack growth at the peak load should also be proportional to the specimen size. However, this speculation has not been justified.

The spatial variation of strength and fracture properties is a common feature of many quasibrittle materials, such as concrete, rock, particulate composites, tough ceramics, etc. Over the past two decades, considerable efforts have been devoted to stochastic numerical simulations of quasibrittle fracture (Grassl and Bažant 2009; Meyer and Brannon 2012; Le et al. 2018; Eliáš and Vořechovský 2020). However, as noted, there is still lack of understanding of the Type 2 size effect in a probabilistic setting. This is what motivates the present study.

Model Description

The present numerical analysis uses a 2D plane stress continuum model. The weak form of the equilibrium equation is discretized by bilinear isoparametric quadrilateral elements, and the resulting nonlinear algebraic system of equations is solved iteratively by the Newton–Raphson method. The focus of this study is on the Mode I fracture, for which a tensile dominant constitutive model is sufficient. We consider an isotropic damage model, in which the stress-strain relation reads

$$\boldsymbol{\sigma} = (1-\omega)\mathbf{C} : \boldsymbol{\varepsilon} \tag{1}$$

where $\boldsymbol{\sigma}$ = stress tensor; ω = damage parameter; $\mathbf{C}$ = elastic stiffness tensor; and $\boldsymbol{\varepsilon}$ = strain tensor. Here, we employ the small strain assumption, i.e., $\boldsymbol{\varepsilon} = \nabla^{\text{sym}} \otimes \boldsymbol{u}$, where $\boldsymbol{u}$ is the displacement vector. The damage parameter ω ranges from zero (intact status) to 1 (fully damaged).

The constitutive model is completed by prescribing a relationship between the damage parameter and the strain tensor. To this end, we consider a history variable κ describing the maximum deformation that the material has ever experienced

$$\kappa = \max_t[\varepsilon_{\text{eq}}(t)] \qquad \varepsilon_{\text{eq}} = \sqrt{\sum_{i=1}^{3}\langle\varepsilon_i\rangle^2} \tag{2}$$

where ε_{eq} = equivalent strain proposed by Mazars (1984); t = loading time; ε_i = principal strains; and $\langle x\rangle$ = Macaulay bracket. The damage parameter is related to variable κ by

$$\omega = \begin{cases} 0 & \kappa \le \varepsilon_0 \\ 1 - \dfrac{\varepsilon_1/\kappa - 1}{\varepsilon_1/\varepsilon_0 - 1} & \varepsilon_0 < \kappa \le \varepsilon_1 \\ 1 & \varepsilon_1 < \kappa \end{cases} \tag{3}$$

where $\varepsilon_0 = f_{\text{t}}/E$ = the strain at which the tensile strength is reached under uniaxial tensile loading; E = Young's modulus; f_{t} = material tensile strength; and $\varepsilon_1 = 2G_{\text{f}}/f_{\text{t}}h$ is the strain at which the material completely loses the load-carrying capacity under uniaxial tension. Here, G_{f} denotes the Mode I fracture energy, and h is the size of the finite element measured in the direction of the maximum principal strain. The present constitutive model yields a linear softening behavior under uniaxial tension [Fig. 1(a)]. The main feature of the constitutive model is that the stress-strain behavior is dependent on the size of finite element. Consider the case of 1D uniaxial tension; we have $\int_0^\infty \sigma_x \mathrm{d}\varepsilon_x = G_{\text{f}}/h$. This relation represents the crack band model (Bažant and Oh 1983; Jirásek and Bauer 2012), which guarantees that, regardless of the element size, the total energy dissipation to completely damage the element is equal to the energy dissipation for propagating a single macrocrack throughout the element. It should be noted that such type of energy regularization is only applicable to the case of fully localized damage, which is the predominant failure mechanism in notched specimens. In more general cases, the structure can experience a transition from diffused damage to localized damage, for which a more general energy regularization model would be needed (Gorgogianni et al. 2020, 2022).

Quasibrittle materials usually contain randomly distributed heterogeneities, which, among other sources, lead to the spatial randomness of material properties. In this study, we consider fracture energy and tensile strength as random variables. For the sake of simplicity, it is assumed that these variables are statistically independent and constant over each finite element. The randomness of G_{f} and f_{t} is described by two independent random fields, $f_{\text{t}}(\boldsymbol{x})$ and $G_{\text{f}}(\boldsymbol{x})$. Thus far, little information is available in regard to the autocorrelation structure of $f_{\text{t}}(\boldsymbol{x})$ and $G_{\text{f}}(\boldsymbol{x})$. Here, we assume that both fields share the same autocorrelation function, where the values of the random variable for elements i and j, whose centroids are located at $\boldsymbol{x}_i$ and $\boldsymbol{x}_j$ respectively, are related by the correlation coefficient

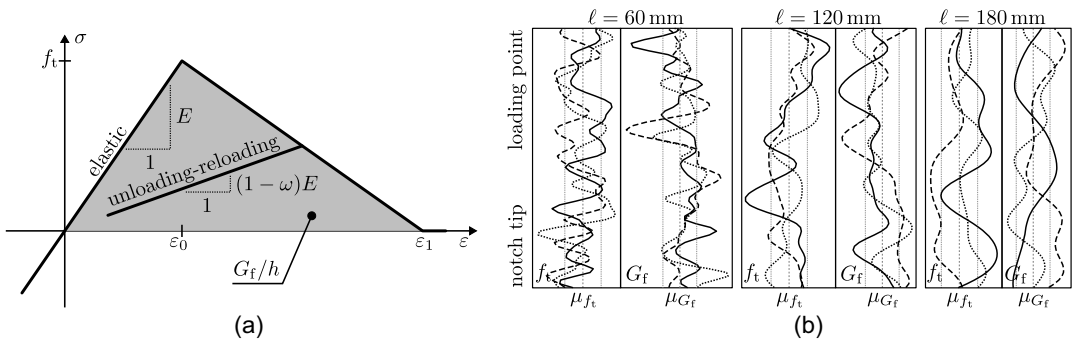

Fig. 1. (a) Stress–strain relationship under uniaxial tension; and (b) realizations of random fields $f_{\text{t}}(\mathbf{x})$ and $G_{\text{f}}(\mathbf{x})$ along the ligament for beam of size $D = 2$ m.

$$\rho(\boldsymbol{x}_i, \boldsymbol{x}_j) = \exp(-\|\boldsymbol{x}_i - \boldsymbol{x}_j\|^2/\ell^2) \tag{4}$$

where ℓ = correlation length. The choices of the autocorrelation functions and possible cross-correlation between $f_t(\boldsymbol{x})$ and $G_f(\boldsymbol{x})$ would surely affect the results quantitatively; however, it would not influence the qualitative scaling behavior of the structural strength.

At any given material point, the random tensile strength and fracture energy are described by a Gaussian distribution. Admittedly, this is an oversimplification since the Gaussian variable extends to negative infinity, while tensile strength and fracture energy must be positive. However, this oversimplification is acceptable for this study for two reasons: 1) the chance that one would sample a negative value of tensile strength or fracture energy is negligibly small (for the distribution functions used in this study, the probabilities of sampling a negative tensile strength and fracture energy are 2.86×10^{-7} and 1.31×10^{-11}, respectively); and 2) the left tails of the probability distributions of tensile strength and fracture energy are unimportant for the prediction of the first- and second-order statistics of the failure load of notched specimens.

As indicated by Eq. (3), the crack band model adjusts the post-peak regime of the stress-strain relationship so as to regularize the energy dissipation. When $G_f \le f_t^2 h/2E$, stress-strain curve would exhibit a snap-back behavior to yield the correct energy dissipation. Such a scenario is difficult to handle computationally. Therefore, in this study whenever the sampled G_f and f_t give a snap-back stress-strain curve. In our simulations, no snapback behavior is encountered for any realizations of $f_t(\boldsymbol{x})$ and $G_f(\boldsymbol{x})$.

The Gaussian random fields of tensile strength and fracture energy are generated by the Karhunen–Loève (K-L) expansion (Karhunen 1946; Spanos and Ghanem 1989; Ghanem and Spanos 2003; Stefanou 2009)

$$f_t(\boldsymbol{x}) = \mu_{f_t} + \sum_{k=1}^{\infty} \sqrt{\lambda_k^{(f_t)}}\, \zeta_k^{(f_t)} \phi_k^{(f_t)}(\boldsymbol{x}) \tag{5}$$

$$G_f(\boldsymbol{x}) = \mu_{G_f} + \sum_{k=1}^{\infty} \sqrt{\lambda_k^{(G_f)}}\, \zeta_k^{(G_f)} \phi_k^{(G_f)}(\boldsymbol{x}) \tag{6}$$

where μ_{f_t}, μ_{G_f} = the mean values the random variables represented by the fields $f_t(\boldsymbol{x})$ and $G_f(\boldsymbol{x})$, respectively; ζ_k^i ($i = f_t, G_f$) = independent standard Gaussian variables; and $\lambda_k^{(i)}$ and $\phi_k^{(i)}(\boldsymbol{x})$ = the eigenvalues and eigenfunctions of the autocovariance function given by the Fredholm integral equation of the second kind

$$\int_\Omega \delta_{(i)}^2 \rho(\boldsymbol{x}_p, \boldsymbol{x}_q) \phi_k^{(i)}(\boldsymbol{x}_q) \mathrm{d}\boldsymbol{x}_q = \lambda_k^{(i)} \phi_k^{(i)}(\boldsymbol{x}_p) \tag{7}$$

where $\delta_{(i)} (i = f_t, G_f)$ = the standard deviation of f_t and G_f, respectively. Eq. (7) is solved numerically. In practice, it suffices to compute only K eigenmodes corresponding to the largest eigenvalues of interest, with the value of $\sum_{k=1}^{K} \lambda_k^{(i)}$ converging with a relative error less than 1%. Fig. 1(b) shows realizations of $f_t(\boldsymbol{x})$ and $G_f(\boldsymbol{x})$ along the midspan of the beam for different correlation lengths.

For a given realization of $f_t(\boldsymbol{x})$ and $G_f(\boldsymbol{x})$, the tensile strength and fracture energy of each finite element are directly obtained from the random values of $f_t(\boldsymbol{x})$ and $G_f(\boldsymbol{x})$ at the centroid of the element. Note that such a local mapping method is applicable when the size of the finite element mesh in the direction of the maximum principal strain is equal to the crack band width (Gorgogianni et al. 2022; Vievering and Le 2024).

Numerical Simulations

We investigate the statistical behavior of the Type 2 size effect through numerical simulations of the failure of a set of geometrically similar notched beams under three-point bending. All beams have a span-to-depth ratio of 2.176, and the initial notch depth is 30% of the beam depth. This study considers 2D geometrical scaling. In the finite element model, all beams have a virtual out-of-plane thickness of 40 mm. The beam depths follow a geometric progression: $D = 2^{k/2}$ m, where $k = -6, -5, \ldots, 6, 7$. The smallest beam has a depth of 0.125 m, and the depth of the largest beam is 11.314 m. The notch width is kept constant (20 mm) for all of the beams.

For notched three-point bend beams, fracture would most likely occur along the ligament at the midspan. Therefore, it suffices to assign nonlinear constitutive model to elements along the ligament above the notch, while rest part of the beam is modeled by elastic elements. Recent studies have shown that, for stochastic simulation of quasibrittle fracture, special care is needed for mapping of the random fields to the finite element meshes in order to suppress the spurious mesh dependence of simulated failure statistics (Le and Eliáš 2016; Gorgogianni et al. 2022; Vievering and Le 2024). To avoid the sophisticated mapping algorithm, we use a fixed mesh of a square shape of size 20×20 mm for the column of elements along the ligament. Note that the width of the finite element mesh is approximately equal to the crack bandwidth. For small-size specimens, the remaining part of the beam is meshed by using the same element size. For the large-size specimens, the mesh size is gradually increasing as we move away from the midspan region (see Fig. 2).

The following elastic material parameters are used: $E = 41.24$ GPa and $\nu = 0.17$ [taken from Hoover et al. (2013)], and the mean tensile strength and fracture energy are $\mu_{f_t} = 3.8$ MPa and $\mu_{G_f} = 65$ N/m^2. The coefficients of variation (CoVs) of f_t and G_f are considered to be 0.15 and 0.2, respectively. The correlation length ℓ is parametrized: $\ell = 60$, 120 and 180 mm. For each correlation length, 500 realizations are computed and statistically analyzed. The finite element simulations were conducted in open-source solver OOFEM (Patzák 2012; Patzák and Rypl 2012).

Results and Discussion

Load-Deflection Responses

We first investigate the effects of specimen size as well as the correlation length of random fields of tensile strength and fracture energy on the load-displacement response. Here, we define the nominal stress by $\sigma = 3PS/2bD^2$ (P is the applied load, S the beam span, b the width of beam in the transverse direction, and D the beam depth), and the relative crack mouth opening displacement (CMOD) by the ratio of CMOD and beam depth ($\delta_{\mathrm{CMOD}} = \Delta_{\mathrm{CMOD}}/D$).

Fig. 3 shows the simulated average $\sigma - \delta_{\mathrm{CMOD}}$ responses for different beam sizes for the case of $\ell = 120$ mm. The $\sigma - \delta_{\mathrm{CMOD}}$ responses simulated by using other correlation lengths exhibit a qualitatively similar behavior. It is seen that the initial elastic response is not affected by the specimen size, as predicted by the theory of elasticity. The subsequent nonlinear behavior is strongly size dependent. The peak nominal stress, also referred to as the nominal strength, decreases significantly with the beam size. This well-known phenomenon is the size effect on the nominal structural

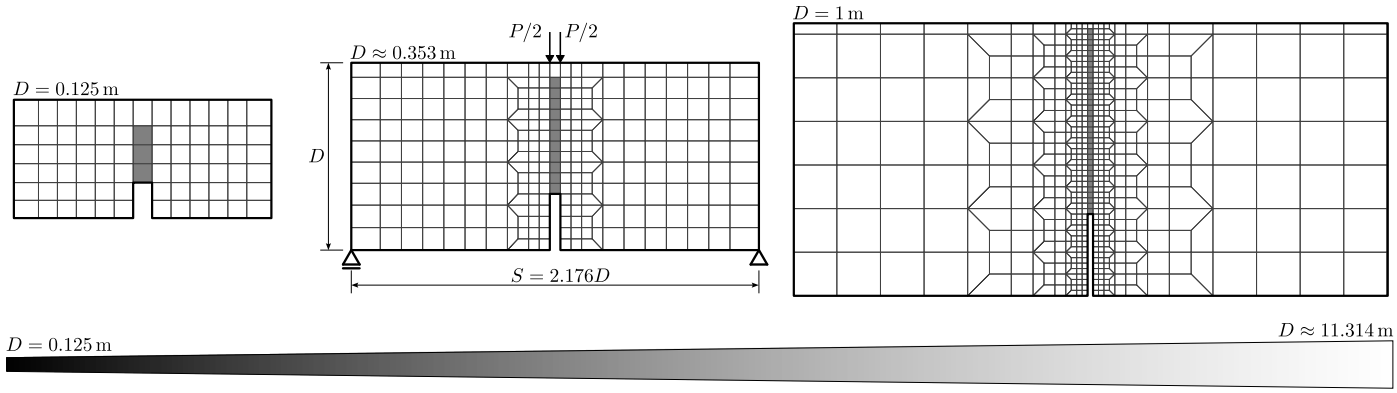

Fig. 2. Finite element mesh of beams of different sizes (note that these beams are not drawn to scale).

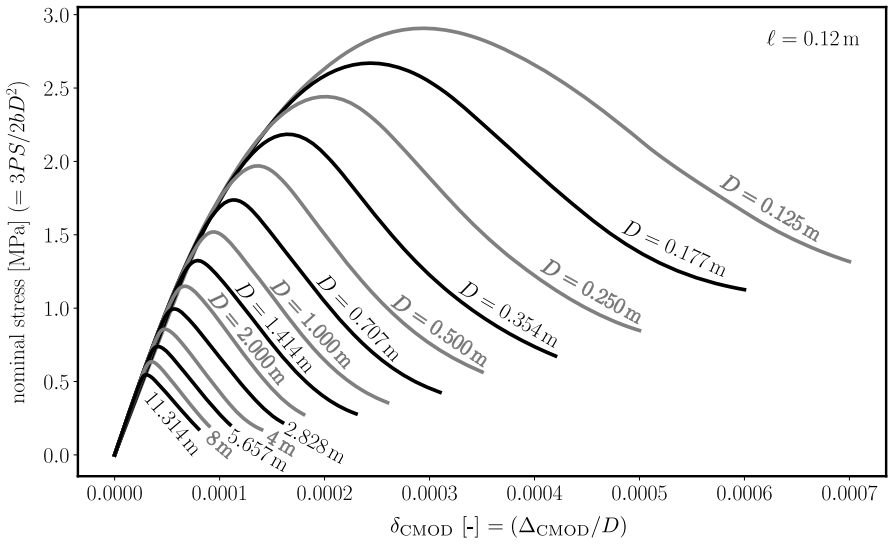

Fig. 3. Simulated mean responses of nominal stress versus normalized crack mouth opening displacement for beams of different sizes and correlation length $\ell = 120$ mm.

strength, which will be discussed in detail in the subsequent section. For the postpeak region of the load-displacement response, it is seen that the small beams exhibit a more gentle softening behavior as compared with the large beams. This indicates that the large beams fail in a more brittle manner as compared with the small beams. As will be discussed, the transition of failure mode as a function of specimen size is further evidenced by examining the stress profile along the ligament.

Fig. 4 presents the effect of correlation length ℓ on the nominalized load-displacement responses for small- and large-size beams. Here, we are interested in the first- and second-order statistics. It is seen that, for the small beams $D = 0.25$ m, the mean and standard deviation of the load-displacement response is not affected by the correlation length. In comparison, for the large beams ($D = 8$ m), the influence of ℓ becomes more discernible. This can be attributed to the fact that, for $D = 0.25$ m, the ligament length of the beam is short and the length of the fracture process zone (FPZ) is comparable or even smaller than the correlation lengths used in the simulation. Therefore, the predicted statistics of load-displacement response are almost the same for $\ell = 0.06$, 0.12, and 0.18 m.

For beams of $D = 8$ m, the mean and standard deviation of the load-displacement response are influenced by the correlation length. This is because, for the large beams, the ligament length is sufficiently large so that the FPZ is fully developed. The length of the fully developed FPZ is larger than the autocorrelation; therefore, the effect of correlation length becomes more pronounced.

Due to the nonlinearity of the damage process, the mean response predicted by the stochastic analysis is different from that predicted by the deterministic analysis using the average material properties. As compared with the deterministic analysis, the mean load-displacement response predicted by the stochastic simulations shows more ductility and a larger amount of energy dissipation. The spatial randomness of strength and fracture energy, on average, leads to the formation of a traction-free crack prior to the peak load. This indicates a larger damage zone leading to a more ductile behavior and more energy dissipation.

It is also seen that simulations with a larger correlation length predict a slightly larger standard deviation of the load-displacement response. This is because the overall load-displacement response is governed by the weighted average of the energy dissipations of all the elements inside the FPZ. A weak spatial correlation of strength

J. Eng. Mech., 2024, 150(6): 04024025

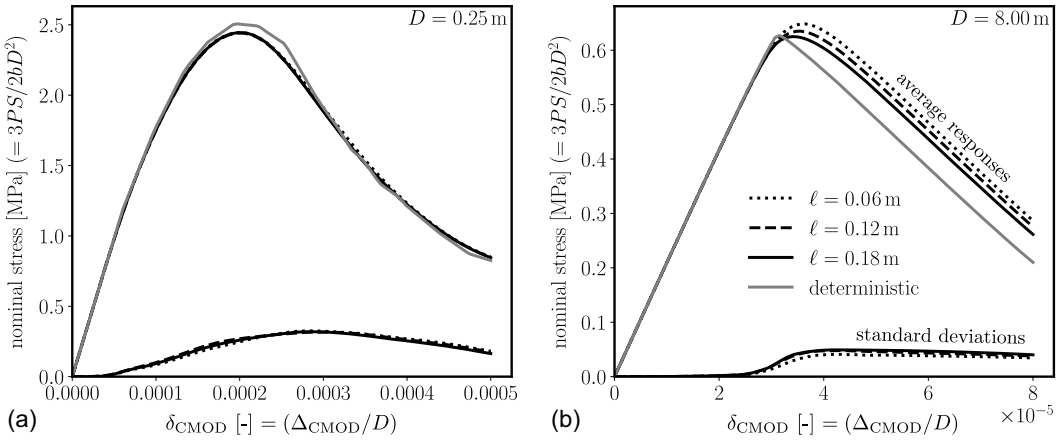

Fig. 4. Statistics of $\sigma - \delta_{\mathrm{CMOD}}$ responses for beams of (a) $D = 0.25$ m; and (b) $D = 8$ m with various correlation lengths.

and fracture energy would result in a smaller statistical variation of the global response.

Stress Profiles along the Ligament

To further investigate the transition of failure modes for different specimen sizes as well as the effect of stochasticity on the failure characteristics, we plot the spatial distribution of tensile stress along the ligament at the peak load for different simulation cases, as shown in Fig. 5. Note that, for each beam size, here we only present the individual results of stochastic analysis calculated from five realizations, which is sufficient for illustrating the key difference between the results of stochastic and deterministic analyses. It is seen that, in the deterministic case, the FPZ is attached at the original crack tip at the peak load. In other words, there is no propagation of the traction-free crack at the peak load, which is consistent with the fact that this specimen is of positive geometry. By comparing the deterministic behaviors of beams of different sizes, it is seen that the length of FPZ first increases with the beam size and eventually approaches a constant value as the beam size becomes sufficiently large. This indicates that the fully developed FPZ has a constant length, which represents an essential length scale governing the size effect on the peak load capacity.

Stochastic results in Fig. 5 are shown only for two correlation lengths; the other case (ℓ = 0.12 m) exhibits a similar behavior. For each beam size, we plot the stress profiles simulated by five arbitrary realizations of random fields of tensile strength and fracture energy. It is seen that, for the small-size specimens, the stress profiles simulated by the stochastic analysis are similar to the deterministic result. This is because for the small-size specimens the FPZ does not exhibit significant spatial variation of the random strength and fracture energy. Consequently, in the limiting case, the random strength and fracture energy in the FPZ can be described as two independent random variables, which do not vary spatially. Clearly, there would not be any traction-free crack growth prior to the peak load.

On the contrary, the stress profiles of the large beams predicted by stochastic analysis are very different from those predicted by deterministic calculation. Stochastic analysis predicts that there could be a discernible extent of traction-free crack growth prior to the peak load. For large beams, the strength and fracture energy exhibit a significant spatial variation. The change of fracture energy ahead the crack tip could be sufficiently large as compared with the increase in the energy release rate due to crack propagation. In this case, a crack would grow at an increasing load.

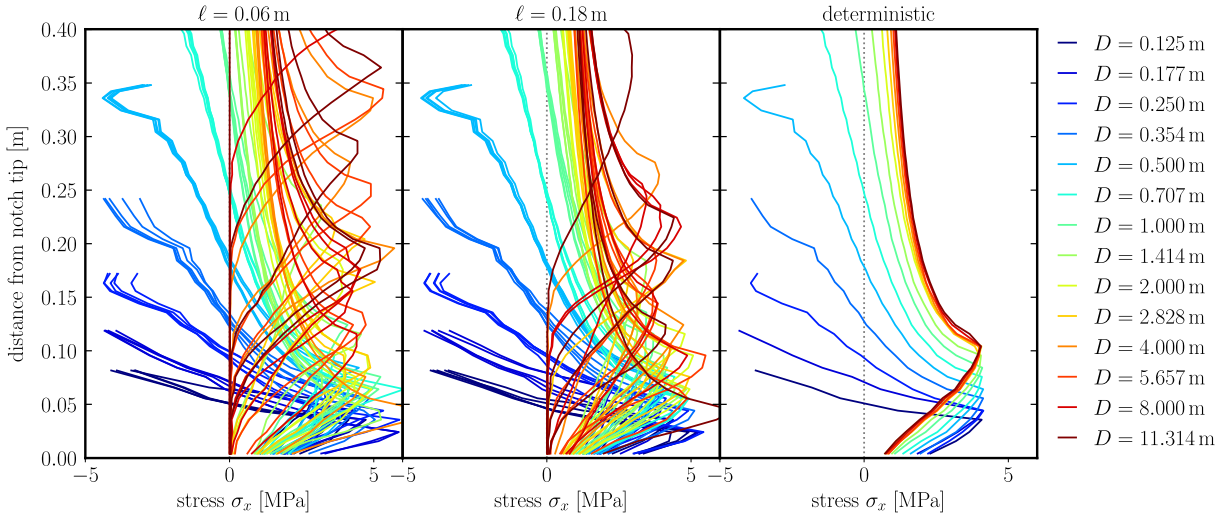

Fig. 5. Stress profiles at the maximum load calculated from five realizations and the stress profile predicted by deterministic analysis.

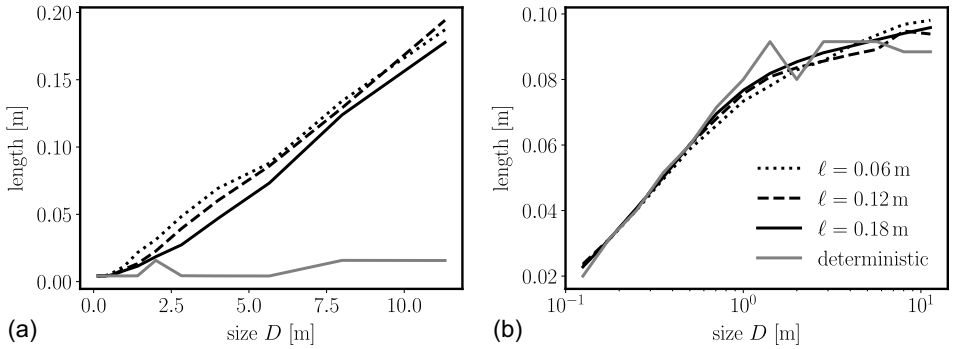

Fig. 6. Fracture behavior of the ligament for different specimen sizes and correlation lengths: (a) average length of the traction-free crack growth; and (b) average length of FPZ.

Fig. 6 presents the mean traction-free crack lengths and FPZ lengths for specimens of different sizes and different correlation lengths. It should be mentioned that Figs. 5 and 6 should not be compared directly. This is because Fig. 5 shows the individual results calculated from five realizations of the underlying random fields, whereas the results plotted in Fig. 6 are the mean behavior calculated from 500 realizations.

Fig. 6(a) shows the average extent of traction-free crack growth. Here, the traction-free crack is defined as the ligament with a damage level exceeding 0.98. As discussed, small-size beams do not experience any traction-free crack growth prior to the peak load. For large beams ($D > 2$ m), there could exist a traction-free crack growth at the peak load; interestingly, the length of crack growth is approximately proportional to the specimen size. This observation has important implications for the size effect on the nominal strength, which will be explained later. It is noted that the extent of the traction-free crack growth is less than 2% of the beam depth.

Fig. 6(b) presents the average FPZ length calculated at the peak load. Here, the FPZ is defined as the region spanning from the point with a damage level of 0.98 to the point where the maximum tensile stress is reached. It is seen that the FPZ grows rapidly with the specimen size until $D \approx 1$ m. When $D > 1$ m, the average FPZ length starts to approach a constant value regardless of the correlation length. The constancy of the average FPZ length has two important implications: 1) the FPZ length represents a characteristic length causing the deviation of the scaling of nominal strength from a power-law form; and 2) the constant average FPZ length implies that the average fracture energy is a constant.

Based on Fig. 6, it is clear that, for large beams, the average size of the total damage zone (traction-free crack growth and the FPZ) predicted by the stochastic analysis is larger than that predicted by the deterministic analysis. This explains the observation that the mean load-displacement response calculated by the stochastic analysis exhibits a larger energy dissipation compared with its deterministic counterpart.

Size Effects on Mean Strength and CoV of Strength

For structural design, arguably the most important design parameter is the peak load capacity. It is convenient to express the peak load capacity in terms of the nominal structural strength σ_N, which is defined by the value of the nominal stress at the peak load. Following the definition of the nominal stress used for Fig. 3, the nominal strength is expressed by

$$\sigma_N = \frac{3P_m S}{2bD^2} \tag{8}$$

where P_m = peak load capacity. Fig. 7(a) presents the mean size effect on the nominal strength in log-log scale. It is seen that the mean size effect curves predicted by the stochastic analysis with different correlation lengths are close to the result of deterministic analysis. This indicates that the mean behavior of Type 2 size effect is largely energetic. Close scrutiny reveals that the stochastic analysis

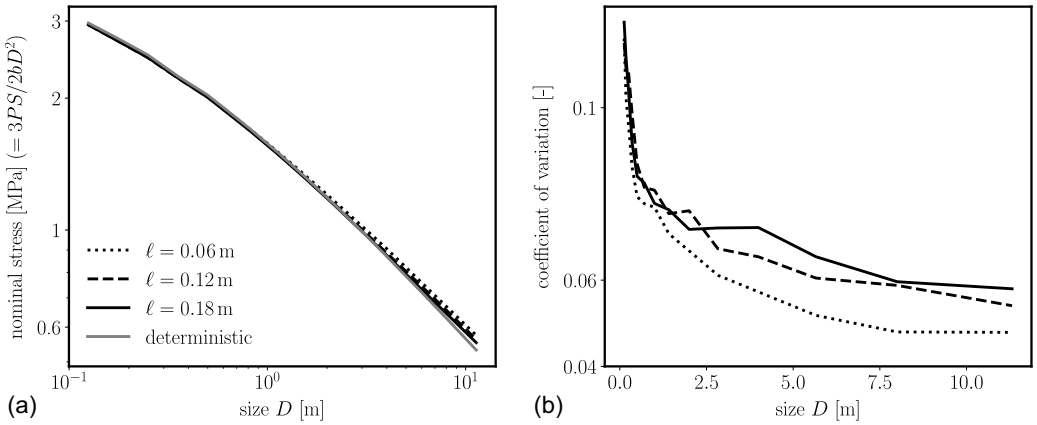

Fig. 7. Size effects on: (a) nominal strength; and (b) strength CoV.

predicts a slightly higher mean nominal strength for the large beams as compared with the deterministic analysis. As the correlation length increases, which indicates less spatial independence in the statistical variation of strength and fracture energy, the result of stochastic analysis gets closer to the deterministic analysis.

In contrast with the mean size effect, the correlation length has a major influence on the size influence on the CoV of nominal strength, as shown in Fig. 7(b). It is seen that the CoV first decreases significantly with an increasing beam size, and it approaches a constant value when the beam size is sufficiently large. Note that the final CoV value at the large-size limit depends on the correlation length. The asymptotic CoV value decreases with a decreasing correlation length, because a smaller correlation length indicates a larger degree of spatial independence of random strength and fracture energy; therefore, there is a stronger averaging effect within the FPZ (Eliáš and Vořechovský 2020). At the large-size limit, the fracture energy governs the peak load, which is essentially the overall energy dissipation of the FPZ. Therefore, less spatial independence of fracture energy diminishes the averaging effect, a larger randomness of the overall energy dissipation and, therefore, a higher CoV of nominal strength.

Based on the foregoing discussion, the size effect on the strength CoV provides a means for determining the correlation length. Direct experimental measurement of correlation lengths of strength and fracture energy is challenging. The result of present simulations indicates that the correlation length could be inferred from the size effect on the strength CoV. It should be pointed out that the study uses the same correlation length for random strength and fracture energy. In a general case, the random fields of strength and fracture energy may have different correlation lengths. Since the nominal strength at the small-size limit is governed by tensile strength, it is conceivable that the correlation length of strength field can be inferred from the strength CoV in the small-size range, while the correlation length of the fracture energy is related to the asymptotic CoV in the large-size range.

Size Effect Model

Based on the foregoing analysis of the simulation results, we develop a size effect model for the mean and CoV of nominal structural strength. In this study, we derive the closed-form scaling relations at small- and large-size limits and then bridge these limits through asymptotic matching.

Size Effect at Small-Size Limit

At the small-size limit, the specimen exhibits quasiplastic behavior when it attains the peak load. In deterministic analysis, the entire ligament experiences uniform tension ηf_t balanced by a concentrated compressive force at the top. By using the engineering beam theory, we can express the nominal strength σ_N by

$$\sigma_N = 3\eta f_t (l_g/D)^2 \tag{9}$$

where η = constant. This constant accounts for the fact that, in the numerical analysis, the elements along the midspan do not experience a uniaxial strain in the horizontal direction. Instead, there exists a small normal positive strain in the vertical direction. Based on the present constitutive model, the maximum tensile stress that can be attained in the horizontal direction would be smaller than f_t.

When the specimen size is sufficiently small, this stress profile does not change with the specimen size. Therefore, the nominal strength is size-independent. Now consider the case of stochastic analysis. When the ligament length is considerably smaller than the correlation length of the random tensile strength ($l_g \ll \ell$), the tensile strengths of material elements along the ligament are fully correlated. Therefore, the randomness of the nominal strength is fully correlated to the random tensile strength via Eq. (9), which implies

$$\mu_{\sigma_N} = 3\eta\mu_{f_t}(l_g/D)^2 \tag{10}$$

$$\omega_{\sigma_N} = \omega_{f_t} \tag{11}$$

When the specimen size is moderately small, the specimen still exhibits quasiplastic behavior, but the ligament length is longer than the correlation length. In this case, the nominal strength is related to the random field of tensile strength by

$$\sigma_N = \frac{6}{D^2}\int_0^{l_g} x f_t(x)\mathrm{d}x \tag{12}$$

where $f_t(x)$ = the random field of f_t along the ligament. By decomposing $f_t(x)$ into its mean and a zero-mean stationary random field, i.e., $f_t(x) = \mu_{f_t} + \widetilde{f}_t(x)$, we can rewrite Eq. (12) by

$$\sigma_N = 3\eta\mu_{f_t}(l_g/D)^2 + \frac{6}{D^2}\int_0^{l_g} x\widetilde{f}_t(x)\mathrm{d}x \tag{13}$$

The mean behavior of the integral $I = \int_0^{l_g} x\widetilde{f}_t(x)\mathrm{d}x$ can be calculated by taking the average of N number ($N \to \infty$) of realizations of $\widetilde{f}_t(x)$

$$\mu_I = \frac{1}{N}\sum_{i=1}^{N}\int_0^{l_g} x\widetilde{f}_{ti}(x)\mathrm{d}x = \int_0^{l_g} x\left(\frac{1}{N}\sum_{i=1}^{N}\widetilde{f}_{ti}(x)\right)\mathrm{d}x \tag{14}$$

Since $\widetilde{f}_t(x)$ is a zero-mean stationary field, we have $\lim_{N\to\infty}\frac{1}{N}\sum_{i=1}^{N}\widetilde{f}_{ti}(x) = 0$. Therefore, $\mu_I = 0$ and $\mu_{\sigma_N} = 3\eta\mu_{f_t}(l_g/D)^2$.

Based on Eq. (13), the standard deviation of σ_N is given by

$$\delta_{\sigma_N} = \frac{6}{D^2}\sqrt{\frac{1}{N}\sum_{i=1}^{N}\left[\int_0^{l_g} x\widetilde{f}_{ti}(x)\mathrm{d}x\right]^2} \qquad (N\to\infty) \tag{15}$$

In general, it is not possible to extract a closed-form solution of the scaling behavior of δ_{σ_N} from Eq. (15) since $\widetilde{f}_t(x)$ is a random field with spatial correlation features. Nevertheless, we can derive the size effect on δ_{σ_N} for the limiting case, where the ligament length is much larger than the correlation length. Here, we divide the ligament into segments of length l_0, where l_0 is several times of correlation length ℓ, so that the total tensile force of each segment is statistically independent. We can now rewrite the integral in Eq. (15) by

$$\begin{aligned}\int_0^{l_g} x\widetilde{f}_{ti}(x)\mathrm{d}x &= \sum_{j=1}^{k}\int_{(j-1)l_0}^{jl_0} x\widetilde{f}_{ti}(x)\mathrm{d}x \\ &= \sum_{j=1}^{k}\int_0^{l_0}[x+(j-1)l_0]\widetilde{f}_{ti}(x+(j-1)l_0)\mathrm{d}x\end{aligned} \tag{16}$$

where $k = l_g/l_0$.

Note that, for the ith realization of the random field of tensile strength, the integral $\int_0^{l_0}[x+(j-1)l_0]\widetilde{f}_{ti}(x+(j-1)l_0)\mathrm{d}x$ represents the resulting moment due to the tensile stress exerted on segment j. Therefore, this moment can be expressed by $[\bar{x}_i^j + (j-1)l_0]\bar{f}_{ti}^j l_0$, where $\bar{f}_{ti}^j = l_0^{-1}\int_{(j-1)l_0}^{jl_0}\widetilde{f}_{ti}(x)\mathrm{d}x$ average tensile stress of segment j, and $\bar{x}_i^j$ = distance from the centroid of the

J. Eng. Mech., 2024, 150(6): 04024025

tensile stress to the top point of the segment. Therefore, Eq. (15) can be rewritten by

$$\delta_{\sigma_N} = \frac{6}{D^2}\sqrt{\frac{1}{N}\sum_{i=1}^{N}\left\{\sum_{j=1}^{k}[\bar{x}_i^j + (j-1)l_0]\bar{f}_{ti}^j l_0\right\}^2} \tag{17}$$

$$= \frac{6}{D^2}\sqrt{\frac{1}{N}\sum_{i=1}^{N}\sum_{j=1}^{k}\sum_{p=1}^{k}[\bar{x}_i^j + (j-1)l_0][\bar{x}_i^p + (p-1)l_0]\bar{f}_{ti}^j\bar{f}_{ti}^p l_0^2} \tag{18}$$

Since the random tensile stress profile of each segment is statistically independent, the resulting moment of each segment must also be statistically independent, which indicates $(1/N)\sum_{i=1}^{N}[\bar{x}_i^j + (j-1)l_0][\bar{x}_i^p + (p-1)l_0]\bar{f}_{ti}^j\bar{f}_{ti}^p = 0$ for $j \neq p$. For the sake of convenience, we normalize $\bar{x}_i^j$ with respect to l_0, i.e., $\bar{x}_i^j = l_0\xi_i^j$. Eq. (18) becomes

$$\delta_{\sigma_N} = \frac{6l_0}{D^2}\sqrt{\frac{1}{N}\sum_{i=1}^{N}\sum_{j=1}^{k}[(\bar{\xi}_i^j)^2 + 2(j-1)\bar{\xi}_i^j + (j-1)^2](\bar{f}_{ti}^j)^2} \tag{19}$$

$$= \frac{6l_0}{D^2}\sqrt{\sum_{j=1}^{k}\mathbb{E}[(\bar{\xi}^j\bar{f}_t^j)^2] + 2(j-1)\mathbb{E}[\bar{\xi}^j(\bar{f}_t^j)^2] + (j-1)^2\mathbb{E}[(\bar{f}_t^j)^2]} \tag{20}$$

where $\mathbb{E}[x]$ = the average value of random variable x. Since the tensile strength is a homogenous random field, the average values of the quantities in Eq. (20) do not depend on the segment number j. Eq. (20) can be further simplified

$$\delta_{\sigma_N} = \frac{6l_0}{D^2}\sqrt{k\mathbb{E}[\bar{\xi}^2\bar{f}_t^2] + k(k-1)\mathbb{E}[\bar{\xi}\bar{f}_t^2] + \frac{2k^3 - 3k^2 + k}{6}\mathbb{E}[\bar{f}_t^2]} \tag{21}$$

Consider the asymptotic case of $l_g \gg l_0$, we only keep the leading term k^3 proportional to D^3 in Eq. (21) and obtain the following scaling relation:

$$\delta_{\sigma_N} \propto D^{-1/2} \tag{22}$$

Based on the foregoing analysis, we conclude that, at the small-size limit, the mean nominal strength is independent of the specimen size, while the CoV of σ_N varies with the specimen size, transitioning from a horizontal asymptote to a power-law of $D^{-1/2}$. The scaling relation $\delta_{\sigma_N} \propto D^{-1/2}$ may not necessarily manifest if the transitional size at which the behavior of the beam deviates from the quasiplastic manner is not much larger than the correlation length ℓ. Meanwhile, the scaling relation of $\delta_{\sigma_N} \propto D^0$ occurs when D is considerably smaller than ℓ. If ℓ is small (e.g., on the order of size of material inhomogeneity), one may not be able to observe the horizontal asymptote in practice. Nevertheless, the understanding of these asymptotic behaviors is useful for constructing the approximate size effect curve over the entire size range.

Size Effect at Large-Size Limit

When the specimen is large as compared with the FPZ, the nominal strength can be calculated based on LEFM. The central concept of LEFM is the Griffith criterion for crack propagation, which relies on the global Mode I fracture energy G_c. Here, we need to distinguish G_c from the fracture energy G_f inputted for the constitutive behavior of finite elements. Note that G_c describes the overall energy dissipation of the FPZ, whereas G_f is related to the energy dissipation for damaging the finite element. In finite element analysis, the FPZ can consist of a number of finite elements. Therefore, G_c can be considered as an average of G_f of the finite elements in the FPZ. For deterministic analysis, there is no difference between G_c and G_f. For stochastic analysis, the mean values of G_c and G_f are the same, while the second-order statistics of G_c and G_f are different. Due to the averaging effect, the CoV of G_c would be smaller than that of G_f.

In this study, we consider spatial variation of random fracture energy $G_c(x)$ along the ligament. The nominal strength and the corresponding crack length must satisfy the following conditions:

$$\mathcal{G}(a_c) = G_c(\Delta a_c) \tag{23}$$

$$\left.\frac{\partial\mathcal{G}(a)}{\partial a}\right|_{a=a_c} = \left.\frac{\partial G_c(x)}{\partial x}\right|_{x=\Delta a_c} \tag{24}$$

where a_c = length of the traction-free crack; and $\Delta a_c = a_c - a_0$. Eqs. (23) and (24) yield the solution of nominal stress σ and the traction-free crack length a_c. Since one may obtain multiple solution pairs of σ and a_c, the nominal strength σ_N is the maximum value of σ among all the solution points. The occurrence of multiple solution pairs for Eqs. (23) and (24) indicates that the load-deflection curve would exhibit multiple local peaks, which reflects the spatial randomness of material properties.

Here, we are interested in the behavior of the asymptotic solution for $D \to \infty$. At this limit, the solution of Eqs. (23) and (24) must occur at the points where $\partial G_c(x)/\partial x = 0$. We write $G_c(x)$ as $G_c(x) = \mu_{G_c} + \tilde{G}_c(x)$, where $\tilde{G}_c(x)$ = a zero-mean stationary random field. We are searching for the stationary points of $\tilde{G}_c(x)$, i.e., $\partial\tilde{G}_c(x)/\partial x = 0$.

Again, we can express $\tilde{G}_c(x)$ by the K-L expansion, i.e., $\tilde{G}_c(x) = \sum_{i=1}^{\infty}\sqrt{\kappa_i}\zeta_i\phi_i(x)$, where ζ_is are independent standard Gaussian variables, and κ_i and $\phi_i(x)$ are the solution of integral equation $\delta_{G_c}^2\int_0^{l_g}\rho(x_1 - x_2, \ell)\phi_i(x_2)\mathrm{d}x_2 = \kappa_i\phi_i(x_1)$, where δ_{G_c} = standard deviation of G_c. It can be shown that the dimensions of κ_i and $\phi_i(x)$ are $(\mathrm{N/m})^2 \cdot \mathrm{m}$ and $\mathrm{m}^{-1/2}$, respectively. Therefore, we have $\kappa_i = \delta_{G_c}^2 l_g\mathcal{F}_i(\ell/l_g)$, $\phi_i(x) = \mathcal{H}_i(x/l_g, \ell/l_g)/\sqrt{l_g}$, and $\tilde{G}_c(x) = \delta_{G_c}\Psi(x/l_g, \ell/l_g)$.

At the LEFM limit (i.e., large structural size), $\ell/l_g \ll 1$, and function Ψ is primarily dependent on x/l_g. If $\partial\tilde{G}_c(x)/\partial x = 0$ has solutions, the solution points must occur at a series of self-similar points, i.e., x_i/l_g = constants $(i = 1, 2, \ldots)$. Following the foregoing discussion, it is clear that, at the peak load, the tip of the traction-free crack lies at one of these solution points. Since l_g is proportional to specimen size D, we can then conclude that the extension of the traction-free crack at the peak load is proportional to the specimen size, i.e., $\Delta a_c = \gamma D$, where γ is a random variable governed by the random profile of $G_c(x)$. Hence, for large-size structures, the average length of the traction-free crack extension at the peak load scales linearly with the specimen size. This is consistent with the simulation result shown in Fig. 6(a).

We can express the energy release rate as $\mathcal{G}(a_c) = \sigma_N^2 D g(\alpha_c)$ where $\alpha_c = \alpha_0 + \gamma$, and $g(\alpha_c)$ is the dimensionless energy release rate function ($\alpha_0 = a_0/D$, and a_0 is the initial crack length). By introducing the random field of $G_c(x)$, Eq. (23) yields

$$\sigma_N = D^{-1/2}\sqrt{\frac{\mu_{G_c} + \delta_{G_c}\Psi(\gamma, \ell/l_g)}{g(\alpha_0 + \gamma)}} \tag{25}$$

For geometrically similar specimens, α_0 is the constant. Based on Eq. (25), the statistics of σ_N is solely governed by the characteristics of $G_c(x)$. Therefore, for a given random field $G_c(x)$, the square root term in Eq. (25) can be represented by a single random variable. What follows is that the mean and CoV of nominal strength σ_N must scale with the specimen size as

$$\mu_{\sigma_N} \propto D^{-1/2} \tag{26}$$

$$\omega_{\sigma_N} \propto D^0 \tag{27}$$

It is interesting to note that the large-size asymptote of the mean size effect predicted by the present model follows the $-1/2$ power-law, which is same as the prediction of the deterministic analysis. However, the deterministic analysis predicts the absence of traction-free crack growth at the peak load, whereas the stochastic analysis predicts, in the mean sense, a finite growth of the traction-free crack.

Transition between Small- and Large-Size Asymptotes

We now construct an approximate size effect model by bridging the small- and large-size asymptotes derived in the previous section. Since the small- and large-size asymptotes derived from the present analysis are same as those predicted by the deterministic analysis, we adopt the deterministic Type 2 size effect equation for the mean size effect

$$\mu_{\sigma_N} = \sigma_0\left(1 + \frac{D}{D_0}\right)^{-1/2} \tag{28}$$

where σ_0 = the mean nominal strength at the small-size limit; and D_0 = length constant governing the transition from the quasi-plastic behavior to the LFEM limit. Based on Eq. (11), we have $\sigma_0 = 3\eta\mu_{f_t}(l_g/D)^2$ for the specimen considered in this study.

The size effect on strength CoV has three asymptotes: 1) no size effect when $D \to 0$; 2) an intermediate asymptote of $D^{-1/2}$; and 3) no size effect when $D \to \infty$. To match these asymptotes, we propose the following size effect equation:

$$\omega_{\sigma_N} = \omega_0\left[1 + \left(\frac{D_b}{D + D_1}\right)^r\right]^{1/2r} \tag{29}$$

where ω_0, D_b, D_1, r = constants; ω_0 = the asymptotic value of strength CoV for very large structures; and D_1 = the intercept between the horizontal small-size asymptote and the intermediate asymptote. It is clear that D_1 must be on the order of the minimum of the correlation length of the random tensile strength and the specimen size at which the failure starts to deviate from the quasi-plastic behavior (i.e., the mean size effect curve starts deviates from the horizontal asymptote). When $D_1 \ll D \ll D_b$, Eq. (29) reduces to $\omega_{\sigma_N} \approx \omega_0(D_b/D)^{1/2}$, which is the intermediate asymptote. As mentioned, depending on the correlation length and beam size at which the quasiplastic behavior diminishes, this intermediate asymptotic may not get manifested.

Fig. 8(a) presents the optimum fitting of the simulated size effects on the mean strength by using Eq. (28). By fitting the mean size effect curve, we have $\sigma_0 = 3.55$ MPa for all three correlation lengths as well as for the deterministic analysis. This is consistent with the fact that the mean value of the nominal strength at the small-size limit is not affected by the random material strength, as shown in Eq. (10). By contrast, the deterministic analysis gives a slightly smaller D_0 value compared with the stochastic analysis. For large beams, the stochastic analysis predicts, in the mean sense, a larger energy dissipation at the peak load and therefore

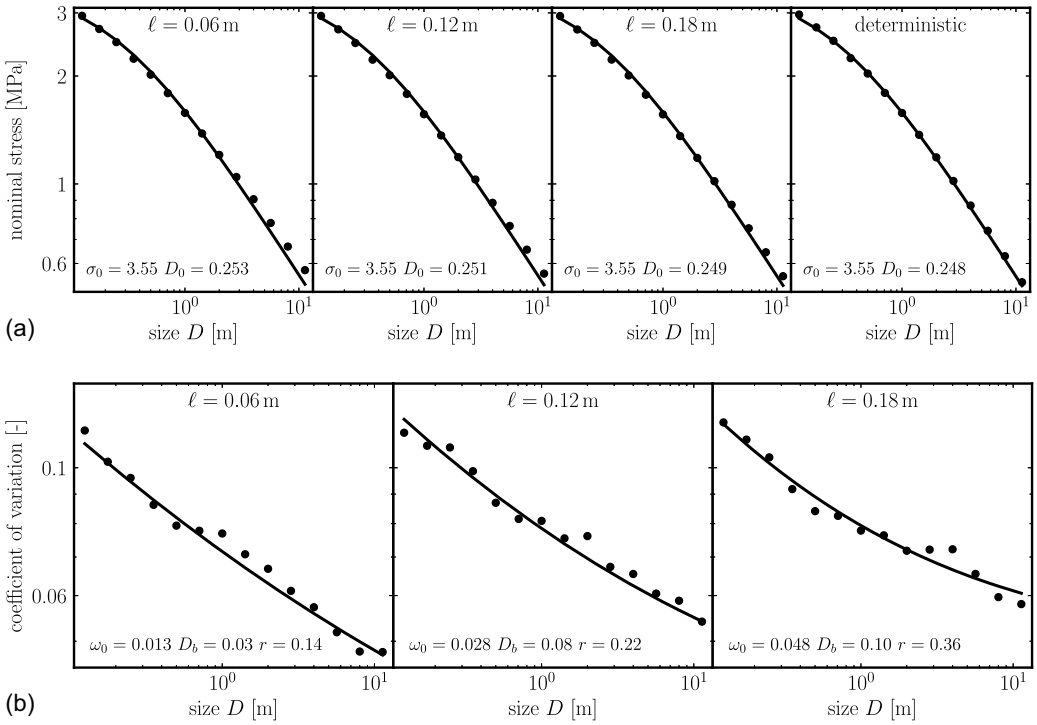

Fig. 8. Optimum fits of size effects on: (a) mean strength; and (b) strength CoV.

J. Eng. Mech., 2024, 150(6): 04024025

a larger mean nominal strength as compared with the deterministic analysis.

Fig. 8(b) shows that the simulated size effects on the strength CoV can be well fitted by Eq. (29). The size range considered in this study does not reach the horizontal asymptote at the small-size limit, Therefore, we have $D_1 = 0$ for all these cases. For the rest of the parameters, we have $\omega_0 = 0.013$, $D_b = 0.03$ m, and $r = 0.14$ for $\ell = 0.06$ m and $\omega_0 = 0.028$, $D_b = 0.08$ m, and $r = 0.22$ for $\ell = 0.12$ m and $\omega_0 = 0.05$, $D_b = 0.25$ m, and $r = 0.46$ for $\ell = 0.18$ m. As discussed, the effect of ℓ on the large-size asymptote of ω can be explained by the fact that the global fracture energy can be viewed as a weighted sum of random fracture energies of individual finite elements in the damage zone. It is also noted that D_b is considerably smaller than D_0. This is because the large-size asymptotes of the size effects on the mean strength and strength CoV should be reached at approximately the same beam size denoted by D_k. Based on Eqs. (28) and (29), D_k/D_0 and $(D_k/D_b)^r$ should be on the same order of magnitude. Since $r < 0.5$, we estimate D_b to be several times smaller than D_0.

The foregoing analysis has important consequences for reliability-based design of quasibrittle structures. Structural design often uses the safety factors, which allow us to ensure a certain level of failure probability based on deterministic analysis (Haldar and Mahadevan 2000). The currently used safety factors, such as the central safety factor and nominal safety factor, rely on the information of the mean and CoV of the nominal structural strength. Figs. 8(a and b) show that the mean strength and strength CoV decreases with an increasing structure size. Therefore, the standard deviation would also decrease as the structure size increases. Though the decreasing standard deviation would improve the structural reliability, the considerable decrease in the mean strength would lead to a significant increase in failure probability. Therefore, to ensure a certain failure probability, the safety factors have to depend on the structure size. Mathematical formulation of the size dependence of safety factors, a topic for future investigation, is of crucial importance for design of large-scale quasibrittle structures.

Conclusions

Through a set of stochastic simulations, the size effects on the mean and CoV of the nominal strength of prenotched quasibrittle structures are investigated. This study leads to the following findings:

1. The size effect on the mean strength can be well described by the Bazant size effect model, which is minimally affected by the stochasticity of the tensile strength and fracture energy. The strength CoV also exhibits a strong size effect. The small-, intermediate-, and large-size asymptotes of the scaling behavior are analytically derived. By asymptotic matching, an approximate size effect equation for the strength CoV is developed.
2. By considering the spatial randomness of fracture energy, the analysis shows that, for large-size specimens, there could exist a traction-free crack propagation at the peak load even if the specimen is of positive geometry. Based on the dimensional analysis, it is shown that the average length of this crack growth is proportional to the specimen size, which agrees with the result of numerical simulation. Consequently, the size effect on the mean structural strength follows a $-1/2$ power-law at the large-size limit (i.e., LEFM limit).
3. Though the correlation length of the random tensile strength and fracture energy has a minimal effect on the size effect on the mean strength, it has a significant consequence for the size effect on the strength CoV, especially at the large-size limit. This indicates that the size effect curve of strength CoV can be used to infer the correlation lengths of random tensile strength and fracture energy, which are difficult to measure directly in the experiment.
4. The demonstrated size effects on the mean and CoV of nominal strength of quasibrittle structures indicate that the size dependence of safety factors must be considered for design of quasibrittle structures.

Data Availability Statement

All data and models that support the findings of this study are available from the corresponding author upon reasonable request.

Acknowledgments

J.-L. Le acknowledges the funding support from the US National Science Foundation (Grant CMMI-2151209) to the University of Minnesota. J. Eliáš acknowledges the funding support from Czech Science Foundation (No. 22-06684K) and support of the internal BUT grant (No. FAST-J-23-8329).

References

Bažant, Z. P. 1984. "Size effect in blunt fracture: Concrete, rock, metal." *J. Eng. Mech.* 110 (4): 518–535. https://doi.org/10.1061/(ASCE)0733-9399(1984)110:4(518).

Bažant, Z. P. 2004. "Scaling theory of quasibrittle structural failure." *Proc. Natl. Acad. Sci. USA* 101 (37): 13400–13407. https://doi.org/10.1073/pnas.0404096101.

Bažant, Z. P. 2005. *Scaling of structural strength*. London: Elsevier.

Bažant, Z. P., and J.-L. Le. 2017. *Probabilistic mechanics of quasibrittle structures: Strength, lifetime, and size effect*. Cambridge, UK: Cambridge University Press.

Bažant, Z. P., J.-L. Le, and M. Z. Bazant. 2009. "Scaling of strength and lifetime distributions of quasibrittle structures based on atomistic fracture mechanics." *Proc. Natl. Acad. Sci. USA* 106 (28): 11484–11489. https://doi.org/10.1073/pnas.0904797106.

Bažant, Z. P., J.-L. Le, and M. Salviato. 2021. *Quasibrittle fracture mechanics: A first course*. Oxford, UK: Oxford University Press.

Bažant, Z. P., and B.-H. Oh. 1983. "Crack band theory for fracture of concrete." *Mater. Struct.* 16 (May): 155–177. https://doi.org/10.1007/BF02486267.

Bažant, Z. P., and S. D. Pang. 2006. "Mechanics based statistics of failure risk of quasibrittle structures and size effect on safety factors." *Proc. Natl. Acad. Sci. USA* 103 (25): 9434–9439. https://doi.org/10.1073/pnas.0602684103.

Bažant, Z. P., and J. Planas. 1998. *Fracture and size effect in concrete and other quasibrittle materials*. Boca Raton, FL: CRC Press.

Eliáš, J., and M. Vořechovský. 2020. "Fracture in random quasibrittle media: I. Discrete mesoscale simulations of load capacity and fracture process zone." *Eng. Fract. Mech.* 235 (Aug): 107160. https://doi.org/10.1016/j.engfracmech.2020.107160.

Fakhimi, A., A. Tarokh, and J. F. Labuz. 2017. "Cohesionless crack at peak load in a quasi-brittle material." *Eng. Fract. Mech.* 179 (Jun): 272–277. https://doi.org/10.1016/j.engfracmech.2017.05.012.

Ghanem, R. G., and P. D. Spanos. 2003. *Stochastic finite elements: A spectral approach*. Minneola, NY: Dover.

Gorgogianni, A., J. Eliáš, and J.-L. Le. 2020. "Mechanism-based energy regularization in computational modeling of quasibrittle fracture." *J. Appl. Mech.* 87 (9): 091003. https://doi.org/10.1115/1.4047207.

Gorgogianni, A., J. Eliáš, and J.-L. Le. 2022. "Mesh objective stochastic simulations of quasibrittle fracture." *J. Mech. Phys. Solids* 159 (Feb): 104745. https://doi.org/10.1016/j.jmps.2021.104745.

Grassl, P., and Z. P. Bažant. 2009. "Random lattice-particle simulation of statistical size effect in quasi-brittle structures failing at crack initiation."

J. Eng. Mech. 135 (2): 85–92. https://doi.org/10.1061/(ASCE)0733-9399(2009)135:2(85).

Haldar, A., and S. Mahadevan. 2000. *Probability, reliability, and statistical methods in engineering design*. New York: Wiley.

Hoover, C. G., Z. P. Bažant, J. Vorel, R. Wendner, and M. H. Hubler. 2013. "Comprehensive concrete fracture tests: Description and results." *Eng. Fract. Mech.* 114 (Dec): 92–103. https://doi.org/10.1016/j.engfracmech.2013.08.007.

Jirásek, M., and M. Bauer. 2012. "Numerical aspects of the crack band approach." *Comput. Struct.* 110 (Nov): 60–78. https://doi.org/10.1016/j.compstruc.2012.06.006.

Karhunen, K. 1946. *Zur Spektraltheorie stochastischer Prozesse. Suomalaisen Tiedeakatemian toimituksia: Sarja A = Series A. 1, Mathematica, physica; 34*. Helsinki, Finland: Suomalainen Tiedeakatemia.

Le, J.-L. 2015. "Size effect on reliability indices and safety factors of quasibrittle structures." *Struct. Saf.* 52 (Jan): 20–28. https://doi.org/10.1016/j.strusafe.2014.07.002.

Le, J.-L., and Z. P. Bažant. 2020. "Failure probability of concrete specimens of uncertain mean strength in large database." *J. Eng. Mech.* 146 (6): 04020039. https://doi.org/10.1061/(ASCE)EM.1943-7889.0001770.

Le, J.-L., Z. P. Bažant, and M. Z. Bazant. 2011. "Unified nano-mechanics based probabilistic theory of quasibrittle and brittle structures: I. Strength, crack growth, lifetime and scaling." *J. Mech. Phys. Solids* 59 (7): 1291–1321. https://doi.org/10.1016/j.jmps.2011.03.002.

Le, J.-L., and J. Eliáš. 2016. "A probabilistic crack band model for quasibrittle fracture." *J. Appl. Mech.* 83 (5): 051005. https://doi.org/10.1115/1.4032692.

Le, J.-L., J. Eliáš, A. Gorgogianni, J. Vievering, and J. Květon. 2018. "Rate-dependent scaling of dynamic tensile strength of quasibrittle structures." *J. Appl. Mech.* 85 (2): 021003. https://doi.org/10.1115/1.4038496.

Luo, W., J.-L. Le, M. Rasoolinejad, and Z. P. Bažant. 2021. "Coefficient of variation of shear strength of rc beams and size effect." *J. Eng. Mech.* 147 (2): 04020144. https://doi.org/10.1061/(ASCE)EM.1943-7889.0001879.

Mazars, J. 1984. "Application de la mécanique de l'endommagement au comportement non linéaire et à la rupture du béton de structure." Ph.D. thesis, Laboratory of Mechanics and Technology, Univ. of Paris.

Meyer, H. W., Jr., and R. M. Brannon. 2012. "A model for statistical variation of fracture properties in a continuum mechanics code." *Int. J. Impact Eng.* 42 (Apr): 48–58. https://doi.org/10.1016/j.ijimpeng.2010.09.007.

Patzák, B. 2012. "OOFEM - An object-oriented simulation tool for advanced modeling of materials and structures." *Acta Polytech.* 52 (6): 59–66. https://doi.org/10.14311/1678.

Patzák, B., and D. Rypl. 2012. "Object-oriented, parallel finite element framework with dynamic load balancing." *Adv. Eng. Softw.* 47 (1): 35–50. https://doi.org/10.1016/j.advengsoft.2011.12.008.

Spanos, P. D., and R. G. Ghanem. 1989. "Stochastic finite element expansion for random media." *J. Eng. Mech.* 115 (5): 1035–1053. https://doi.org/10.1061/(ASCE)0733-9399(1989)115:5(1035).

Stefanou, G. 2009. "The stochastic finite element method: Past, present and future." *Comput. Methods Appl. Mech. Eng.* 198 (9–12): 1031–1051. https://doi.org/10.1016/j.cma.2008.11.007.

Vievering, J., and J.-L. Le. 2024. "Mechanism-based mapping of random fields for stochastic FE simulations of quasibrittle fracture." *J. Mech. Phys. Solids* 186: 105578.